

New solvable model of polymer-chain adsorption at a surface

V. Privman and G. Forgacs

Department of Physics, Clarkson University, Potsdam, New York 13676

H. L. Frisch

Department of Chemistry, State University of New York at Albany, Albany, New York 12222

(Received 4 March 1988)

We solve exactly for the polymer adsorption transition in the two- and three-dimensional directed self-avoiding walk models, by employing a novel transfer-matrix approach. The behavior of the fraction of adsorbed monomers at the threshold and in the high-coverage regime is described in detail, as is the phase diagram of the adsorption transition.

The properties of polymers in the vicinity of walls and interfaces are strongly modified relative to their bulk behavior. For polymer solutions, the study of substrate effects has generated considerable research activity both experimentally and in theory.^{1,2} This interest has been stimulated by important applications, including lubrication, adhesion, surface protection, and coating by polymers.¹ Various aspects of the *single-chain* behavior near walls has also been extensively investigated theoretically by exact calculations,³ general scaling considerations,⁴ Monte Carlo simulations,^{4,5} and enumeration methods,^{6,7} although experimental realization of the idealized single-chain regime seems difficult to accomplish.¹ These studies reveal that for attracting substrates, the chain undergoes an adsorption-desorption transition. For low temperatures, it is pinned at the wall, whereas at higher temperatures a nonadsorbed behavior prevails. Exactly solvable models of this transition were limited to the isotropic Gaussian (non-self-avoiding) random walks.³

In this work we present the exact solution of directed self-avoiding walks (SAW) models for the polymer adsorption transition. Although we consider only a single-chain problem, we believe the results will be useful in scaling studies of dilute polymer solutions as well. In what follows we describe the models, summarize the results, and outline the method of their derivation. Details of the calculations will be published elsewhere.

We define the substrate at the xz plane of the simple cubic lattice [in three dimensions (3D)]. The chain consists of segments (steps) of unit length and is pinned with one of its ends at the origin. This corresponds to the chemically bonded (or grafted⁴) polymers. Only directed models will be considered, for which the x steps are always along the *positive* x direction. This assumption, restricting the number of chain configurations, yields solvable models, while self-avoidance effects are preserved. Both positive and negative y and z steps are allowed, with the restriction that the chain cannot penetrate below the xz plane, i.e., $y \geq 0$. For an L -step walk with l steps in the xz plane at $y = 0$, the attracting wall is modeled by assigning energy $E/kT = -Kl$, with $K > 0$. This corresponds to enhanced probability of making a step in the xz plane, by a factor

$$\kappa = \exp(-E/kTl) = e^K > 1. \tag{1}$$

With the above rules, the projection of a typical walk in the xy plane is shown in Fig. 1. We consider chains in two (2D) and three dimensions (3D). For 2D, Fig. 1 represents a possible walk (in the xy plane).

The behavior of the chains can be analyzed once the partition function

$$Z = \sum_{\text{all walks}} \omega^L \kappa^l \tag{2}$$

is known. Here the fugacity ω controls the average chain length

$$\langle L(\kappa, \omega) \rangle = \omega \frac{\partial \ln Z}{\partial \omega}. \tag{3}$$

The average number of steps *at* the substrate is given by

$$\langle l(\kappa, \omega) \rangle = \kappa \frac{\partial \ln Z}{\partial \kappa}. \tag{4}$$

We will be interested in the fraction of links (steps) adsorbed at the substrate, in the limit of long chains,

$$P(\kappa) = \lim_{\omega \rightarrow \omega_\infty(\kappa)} [\langle l \rangle / \langle L \rangle]. \tag{5}$$

Here $\omega_\infty(\kappa)$ is the value of the fugacity corresponding to $\langle L \rangle \rightarrow \infty$. It will be calculated below

In 2D, we evaluated Z for two models. In the unrestricted model (UM) the difference of the nearest "height variables" y_n can take on any value, $|y_{n+1} - y_n| = 0, 1, \dots, \infty$, when $n = 0, 1, \dots, X$. The assignment of heights y_1, \dots, y_X for the $+x$ steps in a walk ending at $x = X$, is illustrated in Fig. 1, with y_0 and y_{X+1} referring to the y coordinates of the end points. In the restricted model (RM) the difference $|y_{n+1} - y_n|$ can take on only

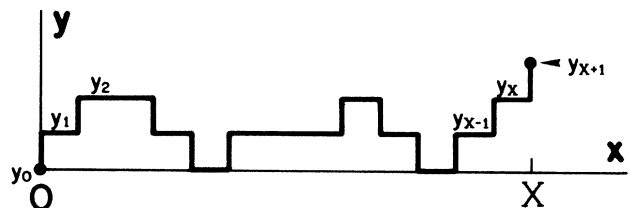


FIG. 1. SAW of $+x$ and $\pm y$ steps, in 2D. The walk shown is *restricted*, with only a single y step at each x , and pinned with its starting point at $y_0 = 0$.

the values 0 or 1. Figure 2 shows $P(\kappa)$ for both models. $P(\kappa)$ vanishes linearly as κ approaches its critical value κ^* from the adsorbed region. [For $\kappa < \kappa^*$, $P(\kappa) \equiv 0$.] In the limit $\kappa \rightarrow \infty (T \rightarrow 0)$, $P(\kappa)$ is given by

$$P_U = 1 - 3\kappa^{-3} - 4\kappa^{-4} - 10\kappa^{-5} + \dots, \quad (6a)$$

$$P_R = 1 - 3\kappa^{-3} - 4\kappa^{-4} - 5\kappa^{-5} + \dots, \quad (6b)$$

for UM and RM, respectively. If Z in (2) is known, the behavior of the fixed- L partition function Z_L , can be evaluated. For large L , in the nonadsorbed regime one expects⁴

$$Z_L^{(1)} \sim \omega_{\infty}^L L^{\gamma_1 - 1}, \quad Z_L^{(11)} \sim \omega_{\infty}^L L^{\gamma_{11} - 1}. \quad (7)$$

Here $Z_L^{(1)}$, $Z_L^{(11)}$ correspond, respectively, to chains with one or both ends fixed at $y=0$. Our calculations yield

$$\gamma_1 = \frac{1}{2}, \quad \gamma_{11} = -\frac{1}{2}. \quad (8)$$

For directed walks without a substrate, the "bulk" exponents γ and ν_{\perp} are 1 and $\frac{1}{2}$, respectively.⁸ [Here γ is defined as in (7), while $\langle y^2 \rangle \sim L^{2\nu_{\perp}}$.] Thus, the surface scaling law⁴

$$2\gamma_1 - \gamma_{11} = \gamma + \nu_{\perp} \quad (9)$$

is satisfied for directed chains. (In the adsorbed regime, the appropriate relation⁴ is $\gamma_1 = \gamma_{11} = \gamma_{(d-1)}$. We find that all three exponents involved are 1.)

As described above, the UM and RM gave very similar results in 2D. With this observation in mind, we considered only the restricted model in 3D. Thus, at most a single $\pm y$ or $\pm z$ step is allowed between any two $+x$ steps, i.e., $(y_{n+1} - y_n)^2 + (z_{n+1} - z_n)^2 = 0$ or 1, where $n=0, 1, \dots, X$, and z_0, z_{X+1} refer to the end points. Note that $y \geq 0$, but any value is allowed for z . We expect that in 3D, the RM will describe the properties of polymer adsorption similarly to the UM. The result for $P(\kappa)$ is shown in Fig. 2. Again, it vanishes linearly as $\kappa \rightarrow \kappa^*$. In the $\kappa \rightarrow \infty$ limit, we find

$$P_{3d}(\kappa) = 1 - 2\kappa^{-1} + 12\kappa^{-2} - 83\kappa^{-3} + \dots, \quad (10)$$

which is quite different from (6).

In what follows we briefly outline our method of calculation. In order to simplify the formulas, we discuss only the 2D case here. Consider a restricted partition function Z_X for all walks having exactly X steps in the positive x direction, i.e., ending at $x=X$. Thus, we have $Z = Z_0 + \sum_{X=1}^{\infty} Z_X$, where $Z_0^{\delta} = \omega/(1-\omega)$ or $Z_0^{\beta} = \omega$ are not interesting and will be omitted below. For $X \geq 1$, we have, for the UM,

$$Z_X = \omega^X \sum_{\{y_n\}=0}^{\infty} \delta_{0y_0} \omega^{\Sigma} \kappa^{\Xi}, \quad \left(\Sigma = \sum_{n=0}^X |y_{n+1} - y_n|, \quad \Xi = \sum_{n=1}^X \delta_{0y_n} \right). \quad (11)$$

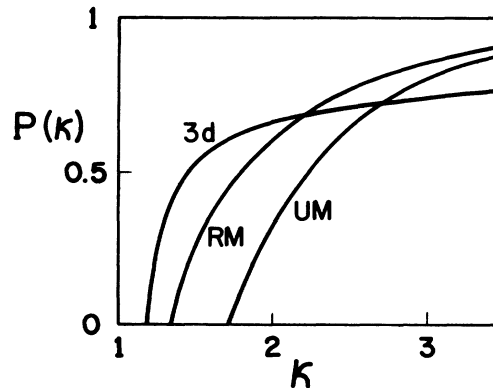


FIG. 2. The adsorption fraction $P(\kappa)$ for the UM and RM in 2D, as well as for the 3D model (see text). The threshold values κ^* are, respectively, $1 + 1/\sqrt{2} \approx 1.707$, $4/3 \approx 1.333$, and $(23 - \sqrt{17})/16 \approx 1.180$ (for UM, RM, and 3D).

Here the pinning of the origin of a chain is accomplished by the factor δ_{0y_0} . (In order to pin both ends at the substrate, one uses $\delta_{0y_0} \delta_{0y_{X+1}}$.) The power of ω in the sum measures the length of all the vertical steps, whereas the power of κ is just l for a given configuration. Z_X can be evaluated by the transfer-matrix method. Indeed, let $T_{nm} = \omega^{|n-m|} \kappa^{\delta_{0n}}$, then the summand in (11) can be represented as

$$\delta_{0y_0} T_{y_1 y_0} T_{y_2 y_1} \dots T_{y_{X+1} y_X} \kappa^{-\delta_{0y_{X+1}}}.$$

Thus,

$$Z_X = \omega^X (V^{(t)} T^{X+1} W), \quad (12)$$

where the (column) vectors V and W account for the end effects, while T is a matrix of T_{nm} . [The superscript (t) denotes the transpose.] Thus, W has entries $W_0 = 1$, $W_{m>0} = 0$ (for the pinned end of a chain). For V , we have $V_0 = \kappa^{-1}$, $V_{m>0} = 1$ (for the dangling end). For chains pinned at both ends, one uses $V_{m>0} = 0$ instead. The transfer matrix for the RM can be constructed similarly, it has elements $(\delta_{0,|n-m|} + \delta_{1,|n-m|}) \omega^{|n-m|} \kappa^{\delta_{0n}}$. In 2D, both T_U and T_R are identical with the transfer matrices of the solid-on-solid models.⁹ (However, the thermodynamic ensemble and Z , are different.) Finally, we get

$$Z = \omega [V^{(t)} T^2 (1 - \omega T)^{-1} W]. \quad (13)$$

Let λ denote the eigenvalues of T . For $\omega \lambda_{\max} = 1$, the partition function Z develops a singularity. (Here λ_{\max} is the largest eigenvalue of T .) This relation defines $\omega_{\infty}(\kappa) < 1$ (see below). For both models, the spectrum consists of a continuous band of eigenvalues (with oscillating eigenvectors), and at most one bound-state (BS) eigenvalue, corresponding to the exponentially localized eigenvector of the form $e^{-\mu n}$ ($\mu > 0$) for $n > 0$.¹⁰ The corresponding equations for μ and λ_{BS} are

$$\cosh \mu = \frac{\lambda(1 + \omega^2) - (1 - \omega^2)}{2\omega\lambda}, \quad \lambda(1 - \omega e^{-\mu}) = \kappa(1 - \omega^2) \quad (\text{for UM}), \quad (14a)$$

$$\cosh \mu = \frac{\lambda - 1}{2\omega}, \quad \lambda - \kappa = \kappa \omega e^{-\mu} \quad (\text{for RM}). \quad (14b)$$

One can show that the solution for λ_{BS} with $\mu > 0$ exists provided $\kappa > \kappa_c$, where

$$\kappa_c^U = (1 - \omega)^{-1}, \quad \kappa_c^R = (1 + 2\omega)/(1 + \omega). \quad (15)$$

For all κ , the continuous spectrum exists¹⁰ for the λ ranges $(1 - \omega)/(1 + \omega) \leq \lambda^U \leq (1 + \omega)/(1 - \omega)$, $1 - 2\omega \leq \lambda^R \leq 1 + 2\omega$. For $\kappa > \kappa_c$, $\lambda_{BS}^U > (1 + \omega)/(1 - \omega)$, $\lambda_{BS}^R > 1 + 2\omega$.

When the bound state exists at $\omega_\infty(\kappa)$, it dominates the singularity in Z (see below), determined then by $\omega\lambda_{BS} = 1$. This equation takes the form

$$\kappa(1 - \omega^2)(1 + \omega - \kappa\omega) = 1, \quad (\text{for UM}), \quad (16a)$$

$$(\kappa - 1)(1 - \kappa\omega) = \kappa^2\omega^4, \quad (\text{for RM}). \quad (16b)$$

The intersection of the curves (15) and (16) then gives the values κ^*, ω^* . The part of the curve (16) for $\kappa > \kappa^*$ describes $\omega_\infty(\kappa)$ for the adsorbed state (localized eigenvector). Figure 3 shows the curve (15), and the appropriate part of (16), for the UM; the curves for the RM (and in 3D) are similar. For $\kappa \leq \kappa^*$ (extended eigenvector), in the nonadsorbed regime, λ_{max} does not depend on κ , and $\omega_\infty(\kappa) \equiv \omega^*$, see Fig. 3. Note that ω^* are given, respectively, by $\sqrt{2} - 1 \approx 0.414$, $\frac{1}{2}$, and $(\sqrt{17} - 1)/8 \approx 0.390$, for the UM, RM, and 3D model.

The substantiation of the above picture, as well as the results for $P(\kappa)$, γ_1 , and γ_{11} quoted earlier, involves the use of the spectral representation of T . In the adsorbed region it is relatively simple since only the bound state must be considered. In the nonadsorbed regime, the calculation involves the eigenspectrum T for *small* wave numbers.¹⁰ These rather lengthy calculations, as well as additional complications arising in 3D, will be presented elsewhere. Finally, we note that $P(\kappa)$ is related to $\omega_\infty(\kappa)$ via

$$P(\kappa) = - \frac{\kappa}{\omega_\infty(\kappa)} \frac{d\omega_\infty(\kappa)}{d\kappa}. \quad (17)$$

In summary, we solved exactly for the single-chain adsorption transition in the 2D and 3D directed SAW models. The behavior at the onset of adsorption is linear [for $P(\kappa)$]. At high coverages, the results for both 2D models are similar (Fig. 2). However, the comparison with the 3D result shows a remarkable suppression of adsorption in the latter case, probably due to large "phase space" available for the chain motion. Our formulation of the adsorption problem in terms of the transfer matrix running parallel to the substrate, will find applications for isotropic SAW models as well, where numerical transfer matrix

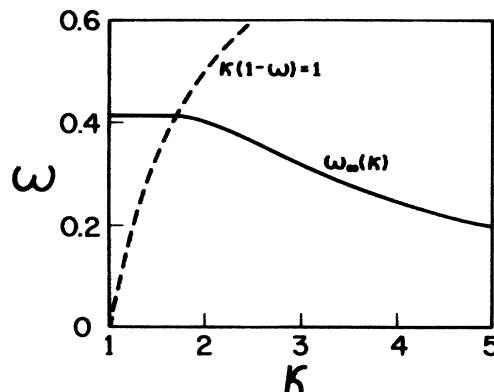


FIG. 3. Phase diagram for the UM. The solid line depicts the function $\omega_\infty(\kappa)$. The broken line indicates the boundary of the adsorbed region (see text).

calculations of bulk properties¹¹ proved very successful.

Directed walk models are relevant for the adsorption of stretched chains.¹² As mentioned, the single-chain regime is difficult to achieve in practice,¹ see, however, Ref. 13. In the nonadsorbed regime, for *fixed* $\kappa < \kappa_c$, some of the directed walk results, e.g., (8), resemble mean-field (Gaussian-walk) theory.^{3,4} Indeed, the "free space" directed walks are Gaussian in their transverse correlations ($\nu_\perp = \frac{1}{2}$).⁸ For $\kappa \gg \kappa_c$, the adsorbed behavior of both directed and isotropic SAW must be quite similar. Near κ_c , as usual in critical phenomena studies, the critical exponent values (i.e., the linearity of the adsorption fraction at the threshold) will differ for isotropic walks, as compared to directed models. To our knowledge, there is no Flory-type theory for the polymer adsorption-desorption transition. In this regard we mention that just as for the bulk (no surface) directed walks,¹⁴ no upper critical dimension exists for the present problem. Studies of other quantities of interest in polymer applications, as well as details of the transfer-matrix calculations, will be presented elsewhere.¹⁵

We wish to thank D. B. Abraham, L. S. Schulman, and N. M. Svrakic for instructive discussions. This research has been supported by the U.S. National Science Foundation under Grants No. DMR-85-15519 and No. DMR-86-01208, and by the Donors of the Petroleum Research Fund, administered by the American Chemical Society, under Grants No. ACS-PRF-18175-G6 and No. ACS-PRF-3519-C5,6. This financial assistance is gratefully acknowledged.

¹Consult reviews by B. Vincent, *Adv. Colloid Interface Sci.* **4**, 193 (1974); A. Takahashi and M. Kawaguchi, *Adv. Polym. Sci.* **46**, 1 (1982).

²D. Ausserre, H. Hervet, and F. Rondelez, *Phys. Rev. Lett.* **54**, 1948 (1985); *J. Phys. (Paris) Lett.* **46**, L929 (1985); *Macromolecules* **19**, 85 (1986); J. M. Bloch, M. Sansone, F. Rondelez, D. G. Peiffer, P. Pincus, M. W. Kim, and P. M. Risenberger, *Phys. Rev. Lett.* **54**, 1039 (1985).

³R. J. Rubin, *J. Chem. Phys.* **43**, 2392 (1965).

⁴For a review, see K. Binder and K. Kremer, in *Scaling Phenomena in Disordered Systems*, edited by R. Rynn and A. Skjeltorp (Plenum, New York, 1985), and references therein. Recent advances have been summarized by P. G. de Gennes, *Adv. Colloid Interface Sci.* **27**, 189 (1987); K. Kremer, *J. Phys. A* **16**, 4333 (1983), reported real-space renormalization-group studies.

- ⁵E. Eisenriegler, K. Kremer, and K. Binder, *J. Chem. Phys.* **77**, 6296 (1982); R. Dickman and C. K. Hall (unpublished).
- ⁶T. Ishinabe, *J. Chem. Phys.* **76**, 5589 (1982); **77**, 3171 (1982); K. Debell and T. Lookman, *Phys. Lett.* **112A**, 453 (1985), and references therein.
- ⁷For general studies of polymers in confined geometries, consult V. Privman, *Phys. Rev. B* **32**, 520 (1985), and references therein.
- ⁸V. Privman and H. L. Frisch, *J. Chem. Phys.* **88**, 469 (1988), and references therein.
- ⁹See, e.g., a review by M. E. Fisher, *J. Chem. Soc. Faraday Trans. 2*, **82**, 1569 (1986). For specific models see, e.g., S. T. Chui and J. D. Weeks, *Phys. Rev. B* **32**, 2438 (1981); J. M. J. van Leeuwen and H. J. Hilhorst, *Physica A* **107**, 319 (1981); G. Forgacs, J. M. Luck, T. M. Nieuwenhuizen, and H. Orland, *J. Stat. Phys.* **51**, 29 (1988).
- ¹⁰In 2D, the continuous eigenvectors are linear combinations of $e^{\pm iq_y n}$ (for $n > 0$) with the wave number $0 \leq q_y \leq \pi$. The eigenvalue $\lambda(q_y)$ can be calculated by replacing $\cosh \mu$ by $\cos q_y$ in the *first* equation (14a), and (14b). In 3D, z is not restricted. As a result, the largest eigenvalues form a continuum of "bound-in- y " states with eigenvectors $e^{-\mu y} e^{\pm iq_x z}$.
- ¹¹D. J. Klein, *J. Stat. Phys.* **23**, 561 (1980); B. Derrida, *J. Phys. A* **14**, L5 (1981).
- ¹²I. M. Ward, *Structure of Properties of Oriented Polymers* (Wiley, New York, 1975).
- ¹³E. A. DiMarzio and M. Bishop, *Biopolym.* **13**, 2331 (1974); see also *Cell Surface Phenomena*, edited by A. S. Perelson, C. DeLisi, and F. W. Wiegel (Marcel Dekker, New York, 1982).
- ¹⁴J. L. Cardy, *J. Phys. A* **16**, L355 (1983).
- ¹⁵V. Privman, G. Forgacs, and H. L. Frisch (unpublished).